Test of the Landau Cutoff of Stimulated Raman Scattering Spectra as an Electron-Temperature Diagnostic in Laser-Produced Plasmas

B. La Fontaine,[2] D. M. Villeneuve,[1] H. A. Baldis,[1],[a] R. P. Drake,[3],[4] and Kent Estabrook[3]

[1]*National Research Council, Ottawa, Ontario, Canada K1A 0R6*

[2]*Institut National de la Recherche Scientifique–Énergie, C.P. 1020, Varennes, Québec, Canada J3X 1S2*

[3]*Lawrence Livermore National Laboratory, Livermore, California 94551*

[4]*University of California, Davis, Livermore, California 94551*

(Received 7 October 1991)

The inference of the electron temperature T_e from the Landau cutoff of backscattered Raman spectra is tested by simultaneous Thomson scattering temperature measurements and compared with results of two-dimensional hydrodynamic computer simulations. If the threshold condition is calculated by using a detailed modeling of the instability, then all three indications of T_e agree. In contrast, the often-used estimate of $k\lambda_{De}\simeq 0.3$ for sizable damping typically overestimates the electron temperature by a factor of 1.5 to 2 in this case.

PACS numbers: 52.70.−m, 52.40.Nk, 94.30.Gm

Laser-produced plasmas are important in a number of applications, including laser fusion [1], x-ray lasers [2], x-ray sources [3], and plasma accelerators [4]. An indirect method of obtaining T_e consists of using the Landau cutoff of the spectrum of stimulated Raman scattering (SRS). SRS is an instability in which the incident laser-light wave decays into a scattering-light wave and a plasma wave [5], with the three waves having frequencies and wave vectors $\omega_0,\mathbf{k}_0$, $\omega_s,\mathbf{k}_s$, and $\omega_e,\mathbf{k}_e$, respectively. In SRS and similar decay instabilities, $\omega_s+\omega_e=\omega_0$ and $\mathbf{k}_s+\mathbf{k}_e=\mathbf{k}_0$. For SRS backscatter discussed here, $k_e \geq k_0$ and, as the plasma density decreases, k_e increases slowly and ω_e decreases. Consequently, the phase velocity of the plasma wave decreases as density decreases until Landau damping becomes large enough to decrease the SRS amplitude. The abrupt onset of Landau damping due to its exponential dependence on T_e allowed Seka *et al.* to propose its use as a T_e diagnostic [6] for experiments with submicron laser wavelengths. Since the inferred values of T_e have often differed by up to a factor of 2 from those calculated using hydrocodes [7], a test by Thomson scattering is of more than general interest. Thomson scattering [8] is a diagnostic that allows a relatively direct measurement of the electron temperature. In laser-produced plasmas, the so-called ion feature of the Thomson scattering spectrum is used to determine T_e [9,10]. We report here the results of experiments that have allowed us to make the first direct comparison of inferences of T_e from the Landau cutoff of the SRS spectrum, Thomson scattering measurements of T_e, and calculations of T_e by a hydrocode.

In this experiment, carried out at the National Research Council of Canada, we studied the SRS instability occurring in plasmas produced by the interaction of a $\lambda_0=1.06$ μm laser pulse with 200-nm- ($\pm 25\%$) thick plastic (CH) targets. The target material was stretched across thin Mylar washers with an inside diameter of 7 mm. The Nd-glass laser system delivered between 50 and 100 J onto a spot of 150 μm ($\pm 20\%$) diameter. Two different pulse lengths were used, 1 and 3 ns FWHM ($\pm 10\%$ in both cases), with a roughly triangular shape. The range of irradiances covered, measured with an uncertainty of $\pm 40\%$, was 9×10^{13} to 7×10^{14} W/cm^2. The exploded CH targets have roughly parabolic density profiles which have a low threshold for SRS, providing favorable conditions for driving the instability. The target thickness was chosen in order to allow the electron density to decrease rapidly enough that the density at which Landau damping occurs would be present near the peak of the laser pulse.

The experimental setup is shown in Fig. 1. The Thomson scattering diagnostic used a $\lambda_{pr}=355$ nm laser probe synchronized with the main laser pulse and of the same duration, focused onto an 80-μm spot in the plasma. The scattered light was collected at 90° from the incident probe and then analyzed by a spectrometer and a streak camera. The spectral resolution was varied with the width of the spectrometer's slit and ranged from 0.5 to

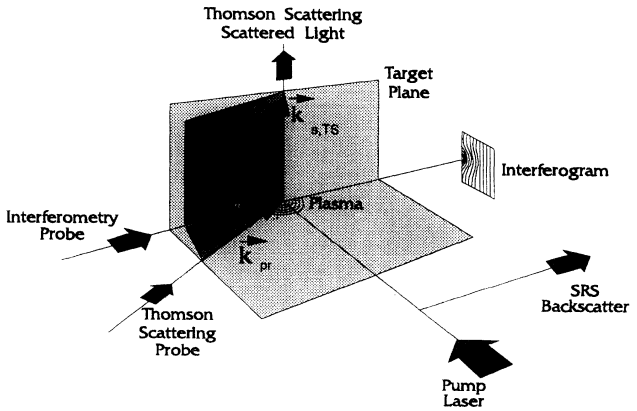

FIG. 1. Schematic of the experiment. A 1.06-μm laser drives the CH foil plasma. The time-integrated backscattered Raman spectrum is obtained with a spectrometer–image-dissector pair. Simultaneously, Thomson scattering measurements and interferometry are performed.

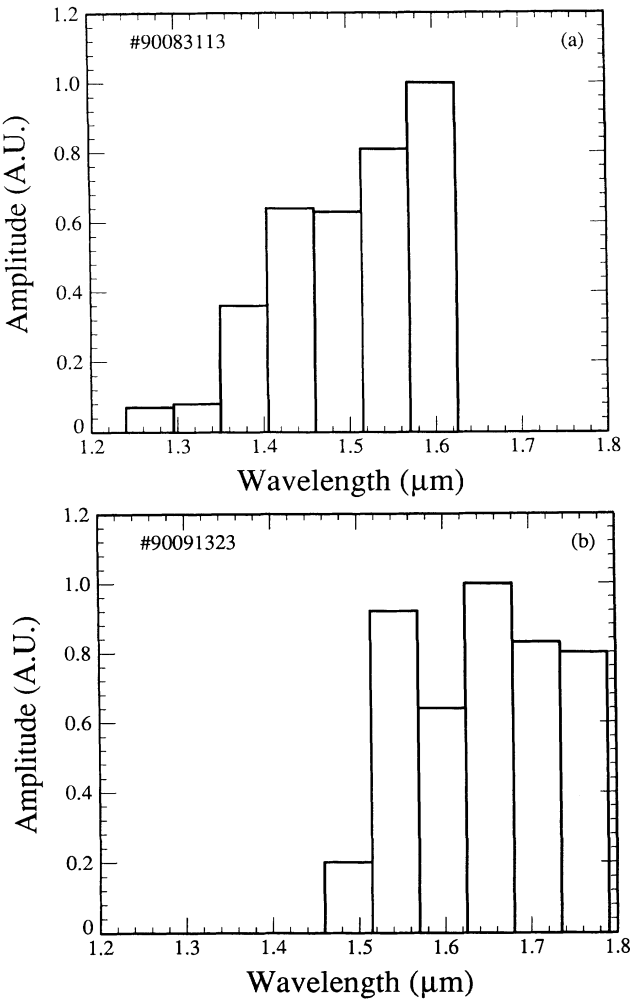

FIG. 2. Typical discrete-channel SRS spectra from 200-nm CH foils irradiated with a 1.06-μm laser pulse. (a) $\tau=3$ ns, $I=9\times10^{13}$ W/cm^2. (b) $\tau=1$ ns, $I=5.9\times10^{14}$ W/cm^2.

0.8 Å. The time resolution was approximately 100 ps and the spatial resolution was $\sim$80 μm, as defined by the spotsize of the probe and by the slit of the spectrometer. The density profiles were measured with a folded-wavefront interferometer using a 355-nm, 100-ps laser-pulse probe, with a magnification from the plasma to the film plate of 23. The SRS light backscattered through the $f/10$ focusing lens was directed into a spectrometer and then to an image dissector [11]. This apparatus focused $\sim$10 channels of spectral information onto a single Au-doped Ge detector with a time delay of 13 ns between channels. The overall spectral resolution of these time-integrated measurements was 55 nm. The spectral window was about 600 nm wide and its placement was varied for the different shots. Two of these discrete-channel SRS spectra from 200-nm CH targets are shown in Fig. 2. The first one [Fig. 2(a)] was obtained at an intensity of 9×10^{13} W/cm^2, using a pulse duration of $\tau=3$ ns, while the other [Fig. 2(b)] was obtained at $I=5.9\times10^{14}$ W/cm^2, with a pulse length of $\tau=1$ ns.

Shortly after the onset of SRS from exploding-foil targets, the spectrum may be broad [7] or narrow [12], depending on the laser intensity relative to the instability threshold. However, both these and other previous data show that the shortest observed wavelength is emitted from the maximum density as this density decays and the Landau damping increases. This result is also expected from theory. The spectrum of the Raman light depends on the densities (n) at which the instability takes place:

$$1-\lambda_0/\lambda_s=\zeta(n/n_c)^{1/2}, \tag{1}$$

where $n_c=10^{21}$ cm^{-3} is the critical density for 1.06-μm lasers, λ_s is the scattered light wavelength, and $\zeta=(1+3k_e^2\lambda_{De}^2)^{1/2}$. In the spectra of Fig. 2, the long-wavelength cutoff is instrumental and the short-wavelength cutoff is due to Landau damping. We define the Landau cutoff to be the wavelength at which the amplitude of the Raman spectrum is less than 20% of the maximum. The cutoffs for Figs. 2(a) and 2(b) are thus respectively 1.32 and 1.49 μm ($\pm$28 nm in both cases). The inferred densities at which sizable damping occurs are $0.04n_c$ ($\pm$20%) at $I=9\times10^{13}$ W/cm^2 [Fig. 2(a)] and $0.08n_c$ ($\pm$20%) at $I=5.9\times10^{14}$ W/cm^2 [Fig. 2(b)].

The simplest way to obtain T_e from the SRS spectrum is to assign a chosen value of $k_e\lambda_{De}$ to the short-wavelength cutoff. We use $k_e\lambda_{De}\simeq0.3$, as is common, corresponding to an electron-plasma-wave phase velocity of approximately 3 times the thermal velocity $v_{th}=(T_e/m_e)^{1/2}$, where m_e is the electron mass. An expression for T_e as a function of the cutoff wavelength can be obtained from the dispersion equation for the waves involved:

$$k_e\lambda_{De}\equiv\left(\frac{k_BT_e}{m_ec^2}\right)^{1/2}\frac{\zeta}{1-\lambda_0/\lambda_s}\left[\left(1-\frac{(1-\lambda_0/\lambda_s)^2}{\zeta^2}\right)^{1/2}+\frac{\lambda_0}{\lambda_s}\left(1-\frac{(\lambda_s/\lambda_0-1)^2}{\zeta^2}\right)^{1/2}\right]\simeq0.3. \tag{2}$$

For a given cutoff wavelength λ_s, this formula is solved for T_e.

A more complex but physically more correct way to calculate T_e from the Landau cutoff wavelength λ_s is to assume that the cutoff corresponds to the SRS going below threshold. In the notation of Williams and Johnston, the threshold for SRS at a density maximum is [13]

$$\Gamma-\tfrac{1}{4}\Gamma^{1/2}-A=0, \tag{3}$$

where $\Gamma=I/I_B$ is the dimensionless growth rate for the collisionless case and $A=A_{coll}+A_{LD}$ is the dimensionless damp-

ing rate. The laser intensity I is normalized by I_B:

$$I_B = \frac{1074\times10^{14}}{(n/n_c)^{1/3}\lambda_{0\mu}^{2/3}} \frac{FT_{\rm keV}^{1/3}}{L_{2\mu}^{4/3}} \ (\mathrm{W/cm^2}) . \quad (4)$$

The collisional attenuation $A_{\rm coll}$ is negligible in the present conditions. $A_{\rm LD}$ is the Landau damping term, given by

$$A_{\rm LD} = \frac{8.45\times10^{4}[(n/n_c)T_{\rm keV}]^{13/6}(L_{2\mu}/\lambda_{0\mu})^{2/3}}{R^{11/3}} \times\exp\left(-\frac{1}{2}\frac{n}{n_c}\frac{511}{R^2T_{\rm keV}}\right), \quad (5)$$

where F and R are functions of the electron density only and are given by Williams and Johnston [13]. $L_{2\mu}$ and $\lambda_{0\mu}$ are respectively the parabolic density scale length and the laser wavelength (both in μm), and $T_{\rm keV}$ is the electron temperature in keV.

In order to use these equations, we need to know the parabolic density scale length. This parameter is provided by both the interferometry and the simulations. For $I=5\times10^{14}$ W/cm^2, with the 1-ns pulse, the measured electron-density profile was fitted with a parabolic profile, $n_e=n_{e0}(1-x^2/L_{2\mu}^2)$. From interferometry, the scale length is $L_{2\mu}=300$ μm ($\pm20\%$) and the maximum density is $n_{e0}=0.08n_c$ ($\pm20\%$), 0.5 ns after the peak of the pulse. The scale length calculated by LASNEX is about 15% shorter than the experimental one. For the plasmas produced by 3-ns pulses, only the simulation result is available. At the peak of the pulse, the maximum density is $n_{e0}=0.04n_c$, and the scale length is $L_{2\mu}=500$ μm. In both cases, the dependence of the threshold on $L_{2\mu}$ is weak. Equations (3) to (5) then give a relation between T_e and n_{e0} (and thus λ_s).

The electron temperature was obtained from Thomson scattering by fitting the theoretical spectra to the experimental spectra. The four parameters used for fitting, T_e, T_i (the ion temperature), and the ion and electron drift velocities, have distinct effects on the calculated spectrum. For the conditions studied, Thomson scattering spectra are dominated by resonance peaks due to the ion acoustic mode in the plasma [9,10]. The separation of these two peaks, $\Delta\lambda_{\rm peaks}$, is determined by the ion acoustic speed, which varies as the square root of T_e. The error bars on the T_e measurements take into account the uncertainty on T_i and n_e, as well as that due to the fitting.

The two-dimensional hydrodynamic simulations were performed with LASNEX [14], using the experimental conditions as input parameters. The exact shape of the pump laser pulse was used. The flux limiter for heat conduction was $f=0.1$. The hydrocode results indicate that the density (n_{e0}) corresponding to the Landau cutoff of the SRS spectra occurs approximately at the peak of the laser pulse. This agrees with the interferometry. The calculated electron temperature and density at that instant are uniform over the 200-μm central region and vary slowly in time. It should be noted here that the simulation results agree well with the Thomson scattering measurements from the same region, for both $I=1\times10^{14}$ and 5×10^{14} W/cm^2.

The results for T_e are displayed in Fig. 3. The Thomson scattering and hydrocode results are shown in both parts of the figure and are seen to be consistent. The values of T_e inferred from the SRS spectra using Eq. (2) are seen to lie typically within a factor of 2 of these results and to overestimate the electron temperature. If we use instead Eqs. (3)–(5) to evaluate T_e, better agreement is obtained, as one would expect. In Fig. 3(b), nearly all the SRS data are consistent with the Thomson scattering data within the measurement accuracy. The error bars

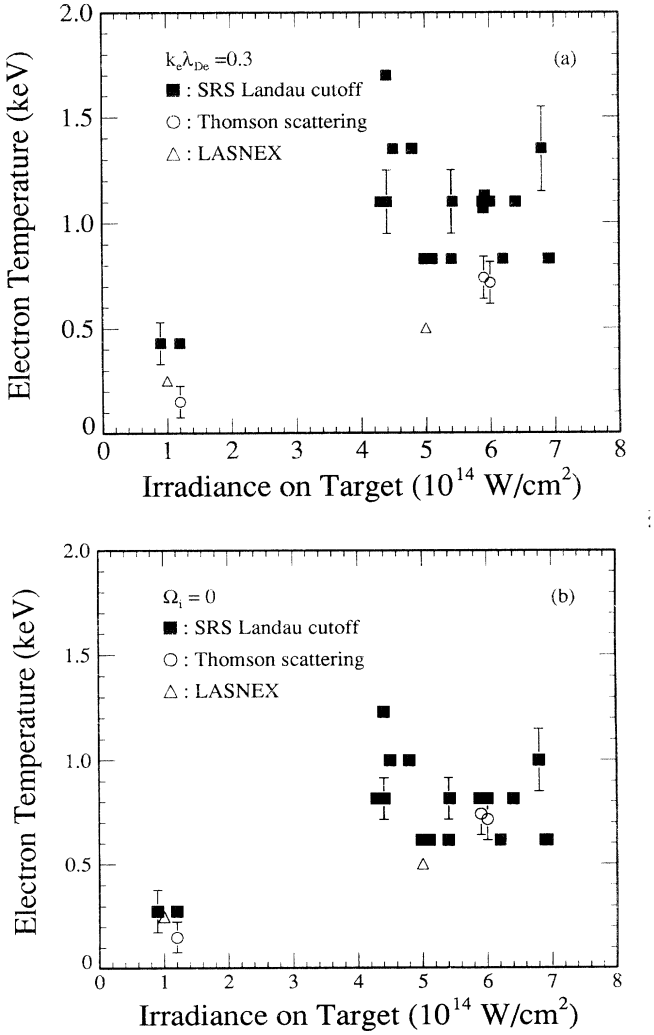

FIG. 3. Measured electron temperature as a function of the irradiance. T_e from the cutoff in the SRS spectrum (■), T_e measured with Thomson scattering at the peak of the pulse (○), and LASNEX estimates at the same instant (△). (a) SRS T_e is deduced from the condition $k_e\lambda_{De}=0.3$. (b) SRS T_e is obtained from the threshold condition $\Omega_i=0$.

on the electron temperature deduced from the Raman data correspond to the width of one channel of the image dissector; the temperature uncertainty due to that of the laser irradiance is half of this amount.

In interpreting the SRS spectra, we have assumed that the plasma was uniform across the 150-μm focal spot of the pump laser. The interferometry does not allow us to be certain of that, because it is not sensitive to small density perturbations. Even if some of the SRS light may originate in filaments, the observed short-wavelength cutoff should correspond to the coldest region in the plasma that is above threshold.

It is worthwhile to point out that, for the present combination of pump intensity and threshold conditions, the criterion $k_e\lambda_{De}\simeq 0.25$, instead of 0.3 as used in Fig. 3(a), would have given results comparable to those obtained with the zero-growth-rate condition [Fig. 3(b)].

In conclusion, a direct comparison of the electron temperature inferred from the Landau cutoff with simultaneous Thomson scattering measurements, and with two-dimensional hydrocode results, was achieved for the first time. The criterion $k_e\lambda_{De}\simeq 0.3$ for "significant" damping is too strong and should be replaced by a better-suited condition for the onset of SRS on parabolic profiles.

The authors would like to acknowledge useful discussions with Professor T. W. Johnston of INRS-Énergie. One of the authors (H.A.B.) would also like to acknowledge Dr. B. F. Lasinski for suggesting this experiment.

---

[a]Present address: Lawrence Livermore National Laboratory, Livermore, CA 94551.

[1] J. Nuckolls, L. Wood, A. R. Thiessen, and G. B. Zimmerman, Nature (London) **239**, 139 (1972).

[2] D. L. Matthews, P. L. Hagelstein, M. D. Rosen, M. J. Eckart, N. M. Ceglio, A. U. Hazi, H. Medecki, B. J. MacGowan, J. E. Trebes, B. L. Whitten, E. M. Campbell, C. W. Hatcher, A. M. Hawryluk, R. L. Kauffman, L. D. Pleasance, G. Rambach, J. H. Scofield, G. Stone, and T. A. Weaver, Phys. Rev. Lett. **54**, 110 (1985).

[3] M. Chaker, H. Pépin, V. Bareau, B. La Fontaine, I. Toubhans, and R. Fabbro, J. Appl. Phys. **63**, 3 (1988).

[4] C. Joshi, W. B. Mori, T. Katsouleas, J. M. Dawson, J. M. Kindel, and D. W. Forslund, Nature (London) **311**, 525 (1984).

[5] C. S. Liu, M. N. Rosenbluth, and R. B. White, Phys. Fluids **17**, 1211 (1974).

[6] W. Seka, E. A. Williams, R. S. Craxton, L. M. Goldman, R. W. Short, and K. Tanaka, Phys. Fluids **27**, 2181 (1984).

[7] R. P. Drake, P. E. Young, E. A. Williams, K. Estabrook, W. L. Kruer, B. F. Lasinski, C. B. Darrow, H. A. Baldis, and T. W. Johnston, Phys. Fluids **31**, 1795 (1988).

[8] J. Sheffield, *Plasma Scattering of Electromagnetic Radiation* (Academic, New York, 1975).

[9] J. E. Bernard, H. A. Baldis, D. M. Villeneuve, and K. Estabrook, Phys. Fluids **30**, 3616 (1987).

[10] B. La Fontaine, H. A. Baldis, D. M. Villeneuve, J. E. Bernard, G. D. Enright, M. D. Rosen, P. E. Young, and D. L. Matthews, in *Proceedings of the Second International Conference on X-Ray Lasers—1990,* IOP Conference Proceedings No. 116 (Institute of Physics, London, 1991), p. 9.

[11] H. A. Baldis, N. H. Burnett, and M. C. Richardson, Rev. Sci. Instrum. **48**, 173 (1977).

[12] C. Labaune, H. A. Baldis, E. Fabre, F. Briand, D. M. Villeneuve, and K. Estabrook, Phys. Fluids B **2**, 166 (1990).

[13] E. A. Williams and T. W. Johnston, Phys. Fluids B **1**, 188 (1989).

[14] G. B. Zimmerman and W. L. Kruer, Comments Plasma Phys. Controlled Fusion **2**, 51 (1975).

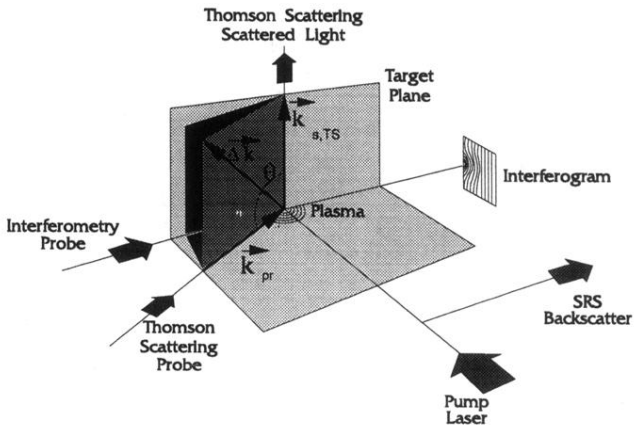

FIG. 1. Schematic of the experiment. A 1.06-μm laser drives the CH foil plasma. The time-integrated backscattered Raman spectrum is obtained with a spectrometer–image-dissector pair. Simultaneously, Thomson scattering measurements and interferometry are performed.